Eksploatacja i Niezawodnosc - Maintenance and Reliability
Volume 29 (2027), Issue 2
https://ein.org.pl
The Polish Maintenance Society

Optimal design of dynamic stiffness matching for gear transmission system of mirror horizontal milling machine based on global sensitivity analysis

Guobin Yan[1], Qiang Cheng[1], Peng Niu[2,*], Guodong Sun[3]

[1] Beijing University of Technology, Machinery Industry Key Laboratory of Heavy Machine Tool Digital Design and Testing Technology, China
[2] State Key Laboratory of Smart Power Distribution Equipment and System, Hebei University of Technology, China
[3] Shandong Institute of Scientific and Technical Information, China
* Corresponding Author: 13881608372@163.com

Received: 25 May 2026
Revised: 10 October 2026
Accepted: 17 October 2026
Online: 12 November 2026

This is an open access article under the CC BY 4.0 license

Abstract

Mirror structured machine tools are critical equipment for aircraft skin machining, where the dynamic stiffness of the transmission system directly affects machining stability and accuracy. To improve the dynamic performance of thin-walled milling systems, this study proposes a parameter analysis and optimization method based on global sensitivity analysis. First, the coupling relationships among key transmission parameters are analyzed, and a dynamic model of the machine tool transmission system is established. Then, the main parameters influencing dynamic stiffness are identified and classified using global sensitivity analysis. Finally, a mirror horizontal milling machine is taken as a case study, and dynamic simulations are conducted to optimize the sensitive parameters. The results show that the proposed method can effectively identify the key factors governing transmission dynamic stiffness, providing a theoretical basis for improving the control accuracy and machining quality of thin-walled components such as aircraft skins.

Keywords: *dynamic stiffness, sensitivity analysis, simulation analysis, matching design*

Article citation:
Yan G, Cheng Q, Niu P, Sun G, Optimal design of dynamic stiffness matching for gear transmission system of mirror horizontal milling machine based on global sensitivity analysis, Eksploatacja i Niezawodnosc – Maintenance and Reliability 2027: 29(2) http://doi.org/10.17531/ein/242317

Highlights

- A dynamic model of the mirror milling machine transmission system was developed.
- Finite element modal predictions agreed with experimental results within 8.2%.
- Sobol analysis identified torque, torsional stiffness, and transmission ratio as key factors.
- MATLAB/Simulink simulations evaluated the effects of key transmission parameters.

1. Introduction

With the rapid development of aircraft manufacturing, the machining of large thin-walled aircraft skins places increasingly stringent requirements on machining accuracy, dynamic stability, and motion-control performance. Mirror horizontal milling machines are important equipment for aircraft skin machining, and the dynamic characteristics of their transmission systems directly affect positioning accuracy and machining stability. Wu et al. applied the Sobol-QMC method to the accuracy analysis of an asymmetric parallel mechanism for aircraft composite skin grinding, demonstrating the value of global sensitivity analysis in the accuracy design of aerospace manufacturing equipment [1]. For geared transmission systems, dynamic stiffness and transmission behavior are closely related to gear-mesh stiffness, inertia, damping, transmission ratio, and servo-drive characteristics [2].

Recent studies have further emphasized the coupled influence of feed-drive mechanics and control on machine-tool performance. Franco et al. investigated the static stiffness of an electronically preloaded rack-and-pinion feed drive and showed that the preload level can significantly affect the stiffness characteristics of the drive system [3]. Wu et al. established dynamic models for the feed system of a five-axis machine tool and evaluated the effects of stiffness and damping variations on its dynamic characteristics [4]. Quan and Zhao reviewed

positioning uncertainty in machine-tool feed drives and highlighted the importance of parameter, disturbance, and model uncertainties in high-precision motion control [5]. Ostad Ali Akbari et al. developed an automated method for identifying machine-tool dynamics for milling stability prediction [6]. For rack-and-pinion drives, Verl and Steinle proposed an adaptive method to compensate transmission errors [7]. Berthold et al. investigated machine-tool dynamics during milling using operational modal analysis [8], while Liu and Altintas demonstrated the position-dependent nature of machine-tool structural dynamics and proposed a data-driven prediction method [9]. These studies indicate that accurate modeling, identification, and parameter matching of feed-drive dynamics are essential for improving machine-tool performance.

At the system level, finite element analysis, modal testing, dynamic modeling, and control-oriented simulation have been widely used to characterize machine-tool dynamics. Sato et al. considered nonlinear friction and process damping in a coupled simulation of machine-tool dynamics and cutting forces [10]. Franco et al. investigated the influence of rack-and-pinion feed-drive control parameters on machine-tool dynamics [11], and Brecher et al. discussed multipoint constraints in machine-tool dynamic modeling [12]. In addition, chatter identification and stability improvement have been studied through speed-varying dynamics identification, feed-drive control tuning, and milling stability prediction [13−15]. Dynamic modeling and performance evaluation of machine tools have also been investigated from the perspectives of kinematic mechanisms, servo-drive control, cutting dynamics, bearing preload, and generalized dynamic response [16−19]. These studies provide important foundations for the establishment and validation of transmission-system dynamic models.

Sensitivity analysis provides an effective way to quantify the contribution of uncertain parameters to system responses. Xu and Gertner extended global sensitivity analysis to models with correlated parameters, providing a theoretical basis for treating coupling among input variables [20]. In recent years, global sensitivity methods have been increasingly applied to gear systems and machine-tool accuracy design. Guo et al. combined dynamic uncertainty analysis with Sobol sensitivity indices to evaluate the influence of machining errors on gear-system dynamic performance [21]. Li et al. used the Sobol method to identify key geometric errors in a large-sized gear hobbing machine while considering the randomness and coupling of error sources [22]. Li et al. further combined Sobol sensitivity analysis with an improved particle swarm optimization algorithm for geometric-error optimization of a horizontal machining center [23]. He and Shi employed global sensitivity analysis to quantify the influence of geometric errors on freeform-surface contour accuracy of a four-axis ultra-precision machine tool [24]. Related studies have also used Sobol sequences, sensitivity analysis, and error modeling for optimization and parameter identification in mechanical and transmission systems [25−28]. These works demonstrate that global sensitivity analysis is suitable for complex nonlinear models involving multiple uncertain and interacting parameters.

Despite these advances, studies focusing specifically on the dynamic-stiffness matching of the gear-rack transmission system in mirror horizontal milling machines remain limited. In such systems, multiple transmission parameters are mutually constrained and coupled, and parameter selection based only on manufacturer data or single-factor engineering experience cannot fully reveal their relative contributions to system dynamic performance. Therefore, this study establishes a dynamic model of the transmission system of a mirror horizontal milling machine and validates the overall machine dynamics through finite element modal analysis and LMS hammer impact testing. On this basis, the Sobol global sensitivity analysis method is used to identify the key parameters affecting transmission dynamic stiffness, and a MATLAB/Simulink model is developed to analyze the effects of rack-and-pinion backlash, coupling type, damping ratio, natural frequency, and motor torque. The sensitive parameters are then matched and optimized to provide a theoretical and engineering basis for improving the dynamic performance and machining accuracy of aircraft-skin milling equipment.

2. Modeling of transmission system for mirror horizontal milling machine

2.1. Rigidity analysis of gear rack transmission in horizontal milling machine

The gear transmission mechanism of the mirror type horizontal milling machine used for aircraft skin processing is analyzed, as shown in Figure 1. The parallel transmission mechanism of the

X-axis is divided into upper and lower parts, with four motors running simultaneously. The upper and lower axes X_1 and X_2 are in parallel.

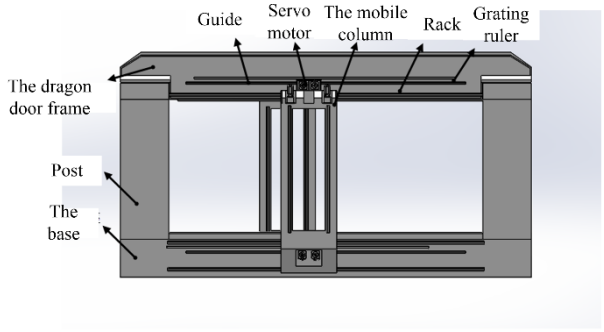


Figure 1. Schematic diagram of the three-dimensional model of the transmission system.

The X-axis is driven by four nominally identical transmission branches. To establish a tractable nominal dynamic model, the following assumptions are introduced: (1) the four servo motors and reducers have identical nominal parameters; (2) the four branches receive synchronized motion commands; (3) the external load is symmetrically distributed so that the branches share the load approximately equally; and (4) differential structural motion among the four branches is neglected in the nominal matching analysis. Under these assumptions, the common-mode response of the parallel drive can be represented by one equivalent branch, and the single-branch model is therefore used for parameter sensitivity and matching design. Possible synchronization errors, branch-to-branch stiffness deviations, preload mismatch and differential vibration modes are not explicitly included. These effects may reduce the actual dynamic stiffness of the complete parallel system and will be considered in a future coupled multi-branch model.

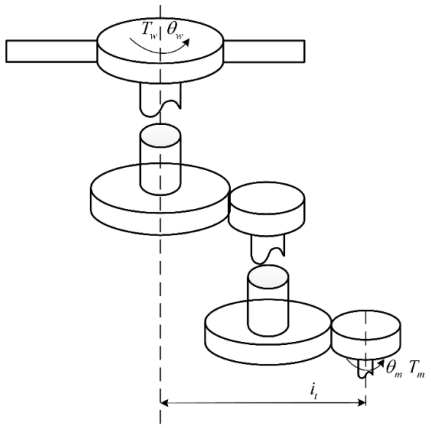


Figure 2. Schematic diagram of chain drive model.

Analyze the branch chains of the transmission system, take out a set of single branch chains from the four motors of the parallel transmission system, and establish a power transmission chain transmission model of the machine tool. The servo motor starts to drive the moving column through the reducer and gear rack mechanism for movement. As shown in Figure 2.

In the model shown in Figure 2, the servo motor transmits the output torque T_m through gear transmission to the end rack and drives the moving column to move in the X-axis direction, achieving feed motion in the X-axis direction. θ_m and T_m represent the motor shaft angle and output torque. θ_w represents the angle of the end gear, which is fed through the load torque T_w on the rack. i_t is the total transmission ratio designed for single chain transmission.

Under the assumption of a rigid body, there is the following relationship:

$$i_t = \frac{\theta_w}{\theta_m} \tag{1}$$

However, due to the presence of many elastic components such as couplings, keys, shafts, and gear pairs in actual transmission systems, equation (1) does not hold. Therefore, the actual relationship between the motor rotation angle and the end gear rotation angle needs to consider the elastic deformation of the components that make up the transmission system. The transmission relationship between the motor shaft rotation angle and the end gear rotation angle can be expressed as:

$$\theta_w = i_t\theta_m + \Delta\theta \tag{2}$$

In the formula, $\Delta\theta$ is the difference between the theoretical and actual rotation angles at the end caused by each elastic element. The stiffness of the entire transmission chain can be obtained from the load torque at this time:

$$k_s = \frac{T_w}{\theta_w - i_t\theta_m} = \frac{T_w}{\Delta\theta} \tag{3}$$

2.2. Dynamic model of transmission system

A research method for establishing a mathematical model of a system based on the internal structure, dimensions, material performance parameters (such as mass, stiffness, damping, etc.), connection conditions, and constraint conditions of the system according to the design diagram of the system structure [29]. Adopting the energy equivalent method for the single branch chain of machine tool transmission, a dynamic model of the

transmission chain is established based on the principle of kinetic energy potential energy equivalence for the torsional stiffness of the shaft.

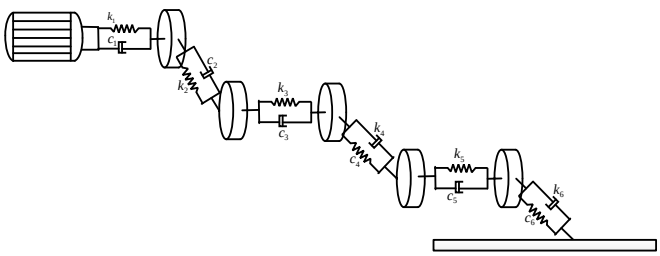


Figure 3. Dynamic model of single branch chain transmission system.

Equivalent the stiffness and inertia of each level of transmission shaft to the input or output shaft end, and treat the entire branch chain as a series of stiffness. Based on the machine tool transmission, the following analysis is made:

Let θ_i， $T_i$respectively represent the input angle and torque; $x_0(t)$ is the output displacement of gear rack transmission; Z_1, Z_2, Z_3, Z_4, Z_5 is the number of teeth of the gear; J_1,J_2,J_3 represents the moment of inertia of axes I, II, and III, respectively; η_1 is the transmission efficiency of gearsZ_1andZ_2, η_2 is the transmission efficiency of gearsZ_3andZ_4, and η_3 is the transmission efficiency between gear Z_5 and rack. d is the diameter of the indexing circle of gearZ_5 , m is the driving mass of the X-axis, B is the viscous damping coefficient, and k is the equivalent torsional stiffness coefficient.

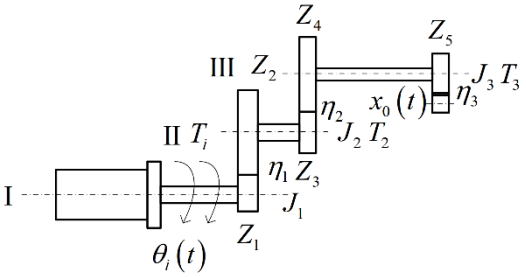


Figure 4. Chain drive system analysis model.

$$k\left[\theta_i(t)-(i_1i_2)\frac{x(t)}{\pi d}\right]=J_1\frac{d^2}{dt^2}\left[(i_1i_2)\frac{x(t)}{\pi d}\right]+\frac{T_2(t)}{i_1\eta_1} \quad (4)$$

$$T_2(t)=J_2\frac{d^2}{dt^2}\left[(i_2)\frac{x(t)}{\pi d}\right]+\frac{T_3(t)}{i_2\eta_2} \quad (5)$$

$$T_3(t)=\left[J_3+\frac{md^2}{4\eta_3}\right]\frac{d^2}{dt^2}\left[\frac{x(t)}{\pi d}\right]+B\frac{d^2}{4\eta_3}\frac{d}{dt}\left[\frac{x(t)}{\pi d}\right] \quad (6)$$

Where：$\frac{x(t)}{\pi d}$——$x(t)$ Equivalent to the angle of rotation on the III axis;

$(i_2)\frac{x(t)}{\pi d}$——$x(t)$ Equivalent to the angle of rotation on the II axis;

$(i_1i_2)\frac{x(t)}{\pi d}$——$x(t)$ Equivalent to the angle of rotation on the I-axis;

$\frac{md^2}{4}$——Equivalent moment of inertia on axis III;

$B\frac{d^2}{4}$——Equivalent damping coefficient of rotational speed on axis III.

Obtained through Laplace transform using torque equation.

$$k\left[\theta_i(s)-(i_1i_2)\frac{X(s)}{\pi d}\right]=J_1s^2\left[(i_1i_2)\frac{X(s)}{\pi d}\right]+\frac{T_2(s)}{i_1\eta_1} \quad (7)$$

$$T_2(s)=J_2s^2\left[(i_2)\frac{X(s)}{\pi d}\right]+\frac{T_3(s)}{i_2\eta_2} \quad (8)$$

$$T_3(s)=\left[J_3+\frac{md^2}{4\eta_3}\right]s^2\left[\frac{X(s)}{\pi d}\right]+B\frac{d^2}{4\eta_3}s\left[\frac{X(s)}{\pi d}\right] \quad (9)$$

Derive the transfer function according to Eq. 7-9.

$$G(s)=\frac{X(s)}{\theta_i(s)} \quad (10)$$

By simplifying Eq. 10, it can be concluded that:

$$G(s)=\frac{X(s)}{\theta_i(s)}=\frac{4\pi dki_1i_2\eta_1\eta_2\eta_3}{Bd^2s+md^2s^2+4\eta_3\left(ki_1^2i_2^2\eta_1\eta_2+J_1i_1^2i_2^2\eta_1\eta_2s^2+J_2i_2^2\eta_2s^2+J_3s^2\right)} \quad (11)$$

Draw a block diagram of the machine tool feed transmission system and simplify the block diagram, ignoring the transmission efficiency of bearings, gears, couplings, etc. during transmission, η_1、η_2、η_3 is equivalent to 1.

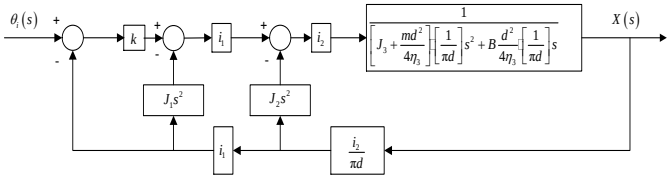


Figure 5. Block diagram of machine tool feed drive system.

Simplify the block diagram of the machine tool feed system and calculate the system transfer function as:

$$G(s)=\frac{X(s)}{\theta_i(s)}=\frac{k(4\pi di_1i_2)}{4i_1^2i_2^2k+Bd^2s+\left(J_1i_1^2i_2^2+J_2i_2^2+J_3+md^2\right)s^2} \quad (12)$$

Equation (12) is further simplified into a second-order dominant-mode model under the following assumptions. First, within the frequency range of interest, the low-order torsional modes of the feed transmission chain dominate the displacement response. Second, the distributed elastic deformations of the shafts, couplings, gears, and rack-and-pinion contacts are represented by the equivalent torsional stiffness k_s and viscous damping coefficient B. Third, local high-frequency bending modes, small bearing deformations, and other higher-order elastic modes are neglected in the reduced-

order model. Finally, the model is linearized around the nominal operating condition; therefore, the effects associated with motion reversal and strongly nonlinear contact behavior are not included in this step.

In this study, the reduced-order model is mainly applied within the frequency range of 0-100 Hz. This range covers the first three structural modes of the whole machine, which are approximately 13-22 Hz, as well as the transmission natural-frequency range investigated in Section 5, corresponding to ω_n=150-600 rad/s, i.e., approximately 24-96 Hz. Therefore, the reduced-order model is intended to describe the dominant low- and medium-frequency transmission dynamics rather than the local high-frequency component modes.

Accordingly, the standard form of the second-order oscillatory element can be expressed as follows.

$$T^2 = J_1 i_1^2 i_2^2 + J_2 i_2^2 + J_3 + md^2 \tag{13}$$

$$K_t = 4\pi d i_1 i_2 \tag{14}$$

Then the system transfer function is obtained as.

$$G(s) = \frac{X(s)}{\theta_i(s)} = \frac{K_t k}{T^2 s^2 + Bd^2 s + (K_t/2\pi \mathrm{d})^2 k} = \frac{(K_t/T^2)k}{s^2 + (Bd^2/T^2)s + (K_t/2\pi dT)^2 k} \tag{15}$$

Available:

$$G(s) = \frac{(k/T^2)K_t}{s^2 + (Bd^2/T^2)s + (K_t/2\pi dT)^2 k} = \frac{K_t \omega_n^2}{s^2 + \xi \omega_n^2 s + (K_t/2\pi d)^2 \omega_n^2} \tag{16}$$

where $\xi = \frac{Bd^2}{k}$, $\omega_n = \frac{\sqrt{k}}{T}$,

K_t — Transmission coefficient of single chain feed transmission system for machine tools,

ξ — Damping ratio of second-order oscillation link,

ω_n — Undamped natural frequency of second-order oscillation link.

Special, there are:

$$G(s) = \frac{\Delta X(s)}{\Delta \theta_i(s)} \tag{17}$$

$$\Delta X(s) = G(s)\Delta\theta_i(s) = \frac{T_w(4\pi d i_1 i_2)}{4 i_1^2 i_2^2 k_s + Bd^2 s + (J_1 i_1^2 i_2^2 + J_2 i_2^2 + J_3 + md^2)s^2} \tag{18}$$

From equations (12) and (18), the response of the end effector can be obtained, and the influence of parameters on the dynamic stiffness of the transmission mechanism can be analyzed. The dynamic stiffness used in this study is defined based on the disturbance force-displacement relationship at the rack output end. The tangential force acting on the rack is expressed as Eq. (19):

$$F_w(s) = \frac{2T_w(s)}{d_w} \tag{19}$$

where $F_w(s)$ denotes the tangential force acting on the rack, $T_w(s)$ is the load torque at the output gear, and d is the pitch-circle diameter of the output gear. Accordingly, the dynamic compliance of the transmission system is defined as Eq. (20), and the dynamic stiffness is defined as Eq. (21).

$$C_d(j\omega) = \left|\frac{\Delta X(j\omega)}{F_w(j\omega)}\right| \tag{20}$$

$$K_d(j\omega) = 1/C_d(j\omega) = \left|\frac{F_w(j\omega)}{\Delta X(j\omega)}\right| \tag{21}$$

In these equations, $\Delta X(j\omega)$ denotes the displacement response at the output end of the transmission system, ω is the excitation angular frequency, and j is the imaginary unit. Therefore, under the same disturbance-force input, a smaller displacement response corresponds to a higher dynamic stiffness. In the subsequent Sobol sensitivity analysis, the same disturbance input is applied to all parameter samples, and the amplitude of the output displacement response is used as an indirect evaluation index of the dynamic stiffness. Thus, the sensitivity of the transmission parameters to the displacement response reflects their influence on the dynamic deformation resistance of the transmission system.

3. Dynamic and static test analysis of horizontal milling machine

The dynamic characteristics of the horizontal milling machine transmission system were analyzed using finite element analysis method and LMS hammer vibration test method. The static and dynamic analysis of the horizontal milling machine was carried out by comparing the results of the test method and simulation. The basic transmission structure of the transmission chain was determined, and the initial selection of transmission components was completed.

3.1. Finite element modal analysis of the entire machine

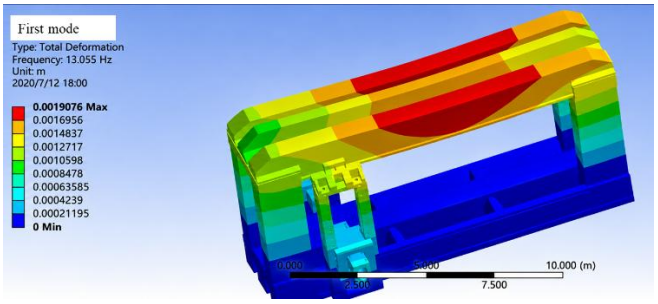
Firstly, draw a 3D model of each component of the overall gantry machine tool, set the scale of the machine tool, and conduct interference checks during the assembly process. After the assembly of the entire machine is completed, select the materials. Analyze the dynamic and static tests of the entire machine and the functional components of each transmission system, and select the appropriate natural frequency range of the

transmission system. Priority should be given to selecting the materials for each component of the machine tool as follows:

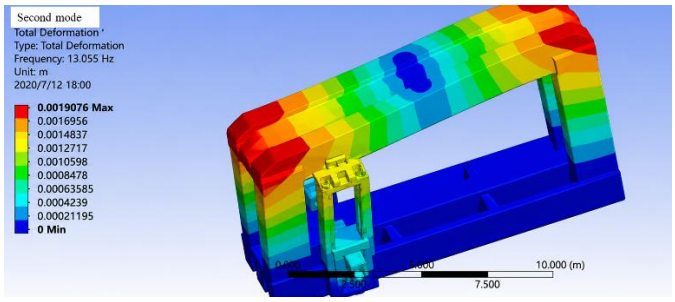
Table 1. Material of main components of mirror horizontal milling machine tool.

Name	Material
Mobile column tool magazine side	Q235A
Moving column support side	Q235A
Retroflex saddle	Q420
Circular support side sliding saddle	Q420
Supporting side sliding pillow	QT700
Milling side sliding pillow	QT700
Fixed frame type gantry	Q355

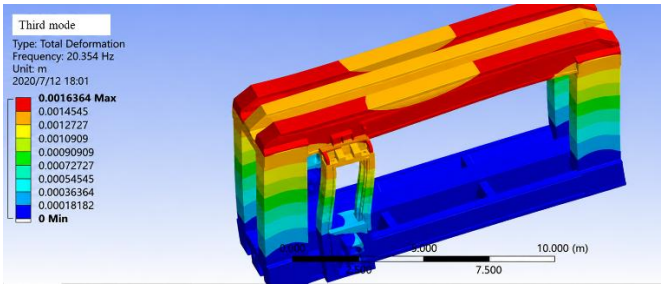
Set grid division and obtain simulation results as shown in the following figure 6.



(a)



(b)



(c)

Figure 6. The first three-order vibration shape diagram of the whole machine simulation analysis.

3.2. Whole machine hammer impact mode test

After completing the simulation of the three-dimensional model of the entire machine, on-site dynamic testing experiments are conducted to obtain the test modes and damping ratios of the machine tool, as well as the actual vibration modes of the machine tool during the testing process. And compare the obtained vibration mode diagram and modal analysis structure with the finite element simulation results to verify the reliability of the obtained natural frequencies.

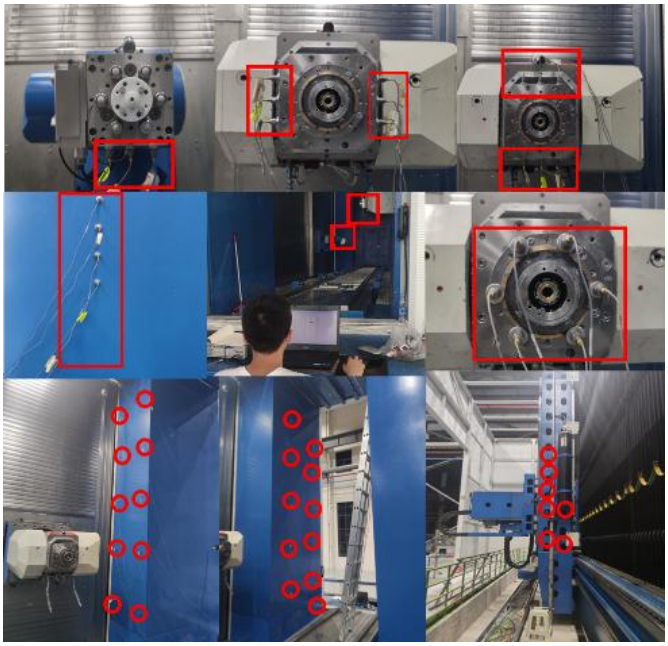


Figure 7. Sensor layout diagram of the machine tool.

Table 2. Comparison table of natural frequency of whole machine.

Order	1	2	3
Simulation calculation frequency（Hz）	13.055	19.34	20.354
Test frequency（Hz）	13.53	18.75	22.17
Difference（Hz）	0.475	0.59	1.816
error（%）	3.511	3.147	8.191

The relative frequency error is calculated as $\varepsilon_f = \frac{|f_{\text{test}} - f_{\text{FE}}|}{f_{\text{test}}} \times 100\%$, where f_{test} is the natural frequency obtained from the LMS hammer impact test, and f_{FE} is the natural frequency obtained from finite element modal analysis. The errors of the first three modes are 3.511%, 3.147% and 8.191%, respectively. The first two modal frequencies show close agreement between the finite element model and the hammer-impact test, whereas the third-mode deviation is relatively larger. This difference is mainly attributed to the idealization of joint and contact stiffness in the finite element model, simplification of boundary conditions, uncertainty in material and damping parameters, and experimental factors such as sensor attachment, impact direction and modal-parameter identification. Nevertheless, all three frequency deviations remain below 10%, and the measured and simulated mode shapes exhibit the same dominant deformation trends. The model is therefore

considered adequate for the low-order dynamic trend analysis and subsequent transmission-parameter matching in this study, while it is not intended as a high-precision predictor of higher-order local modes.

4. Sensitivity analysis of Sobol based on gear transmission

Starting from the sensitivity of machining accuracy, existing sensitivity calculation methods are insufficient to match the dynamic stiffness calculation of machine tool transmission systems. There are still many problems with the commonly used inertia sensitivity matching design calculation methods, among which the two most critical problems are: firstly, there is no systematic calculation method for reference; Secondly, the selection of servo motors mainly relies on the parameters provided by manufacturers, and cannot be adjusted according to the dynamic changes of the machine tool.

When designing parameter matching for the dynamic stiffness of machine tools, sensitivity analysis is used to rank the various parameters that affect the machine tool's sensitivity. The parameters that have a significant impact on the machine tool's transmission system are analyzed and selected to obtain the optimal parameter ratio for achieving the optimal dynamic stiffness of the machine tool.

Analyze the dynamic model of the gear transmission of the established horizontal milling machine. The dynamic model of the transmission system is determined by the parameters of the servo motor, gear, and worktable execution mechanism. There are many input parameters, and the parameters that affect the stability of the gear transmission are relatively complex. Sensitivity classification using Sobol sensitivity analysis method to analyze the impact of different parameters on gear transmission stability.

Sobol method is a variance-based Monte Carlo method for machine tool analysis, which relies on dynamic models incorporating equivalent inertia parameters.

$$f(\Delta x) = f(T_i, d, m, B, k, i_1, i_2, J_3) \tag{22}$$

where $j_1 = j_3/({i_1}^2 {i_2}^2)$ and $j_2 = j_3/{i_2}^2$ are dependent equivalent inertia parameters derived from the transmission ratios.

Set the parameter model of the machine tool for the dynamic stiffness of the machine tool:

$$f(\Delta x) = f(\Delta x_1, \Delta x_2, \cdots \Delta x_k) \tag{23}$$

where $k \in [1,2,\cdots 10]$.

Given the input parameter space domain of a dynamic model

$$X^k = (\Delta x/0 \le \Delta x_i \le 1, i = 1,2,\cdots,k) \tag{24}$$

Decompose the functions that affect the dynamic stiffness of machine tools into multidimensional function superposition combinations:

$$f(\Delta x) = f_0 + \sum_i f(\Delta x_i) + \sum_{i<j} f_{ij}(\Delta x_i, \Delta x_j) + \cdots + \sum_{i<j} f_{ij}(\Delta x_1, \Delta x_2, \ldots, \Delta x_k) \tag{25}$$

In the formula, f_0 is a constant, and the integration of the $2^k - 1$sub term superposition function in the variable's domain is 0, and the sub term functions are orthogonal to each other, which can be expressed as.

$$\int_0^1 f_{i1,\cdots is}(\Delta x_{i1}, \Delta x_{i2}, \ldots, \Delta x_{is}) d\Delta x_{in} = 0,\ (1 \le n \le s) \tag{26}$$

$$\int_{X^k} f_{i1\cdots is} f_{j1\cdots jm} dX = 0, \quad (i_1, i_2, \cdots, i_s) \ne (j_1, j_2, \cdots j_m) \tag{27}$$

$$\int_{X^k} f(X)\, dX = 0 \tag{28}$$

Where $dX = d\Delta x_1 d\Delta x_2 \cdots = \Pi d\Delta x_n$.

By analyzing equations (26) - (28) the multiple integrals of each sub term function can be obtained. It can be expressed as:

$$\int_{X^k} f(X)\, \Pi d\Delta x_n = f_0 \tag{29}$$

$$\int_0^1 \cdots \int_0^1 f(X) \prod_{n \ne i} d\Delta x_n - f_0 = f_i(\Delta x_i) \tag{30}$$

$$\int_0^1 \cdots \int_0^1 f(X) \prod_{n \ne i,j} d\Delta x_n - f_0 - f_i(\Delta x_i) - f_j(\Delta x_j) = f_{ij}(\Delta x_i, \Delta x_j) \tag{31}$$

And so on, the remaining sub term functions can be used to obtain all the sub terms.

The total variance of a uniformly distributed function can be expressed as:

$$D = \int_{X^k} f^2(X)\, \Pi d\Delta x_n - f_0^2 \tag{32}$$

According to formula (22), the partial difference of each sub term can be solved:

$$D_{i1,\cdots is} = \int_0^1 \cdots \int_0^1 \int_{X^k} f_{i1\cdots is}^2(\Delta x_{i1}, \cdots, \Delta x_{is})\, \Pi d\Delta x_n \tag{33}$$

Squaring formula (22) first and then integrating it can be expressed as:

$$D = \sum_i D_i + \sum_{i<j} D_{ij} + \cdots + D_{1,2,\cdots,k} \tag{34}$$

The sensitivity of machine tool transmission parameters to dynamic stiffness can be expressed as:

$$S_{i1,\cdots is} = \frac{D_{i1,\cdots is}}{D} \tag{35}$$

$S_i$is the main influence of parameterΔx_i on the output.

$$S_{Qi} = \frac{\sum_{1 \le s \le n} D_{i1\cdots is}}{D} \tag{36}$$

In the formula, S_{Qi} represents the global sensitivity of parameter Δx_i, indicating the degree to which parameter Δx_i affects the model output after considering the connections between various parameters.

In the given interval and probability distribution of parameter changes, two independent samples are taken of the parameter variables that affect dynamic stiffness to obtain two sampling matrices E and F. Taking K sampling times, the following relationship can be obtained.

$$\frac{1}{K}\sum_{n=1}^{K} f(E)_n \approx f_0 \tag{37}$$

$$\frac{1}{K}\sum_{n=1}^{K} f^2(E)_n - f_0^2 \approx D \tag{38}$$

$$\frac{1}{K}\sum_{n=1}^{K} f(E)_n f(F_i)_n - f_0^2 \approx D_i \tag{39}$$

$$\frac{1}{K}\sum_{n=1}^{K} f(E)_n f(E_i)_n - f_0^2 \approx D_{-i} \tag{40}$$

Where E_i,F_i represent the exchange of the second column of the two matrices in the sampled sample. Calculate the sensitivity of the parameters based on equations (37) to (40) and determine the degree to which each parameter of the machine tool transmission system affects the dynamic stiffness. Given the variation interval and probability distribution of each parameter, Monte Carlo sampling is used to extract the required samples twice, with a sampling frequency of 5000 times. Two sampling matrices **E** and **F** are generated to represent the extracted parameters. A sample size of K = 5000 is adopted as a compromise between computational cost and screening resolution. For Monte Carlo estimators, the nominal sampling-uncertainty scale decreases approximately with $K^{\frac{-1}{2}}$thus K = 5000 corresponds to an order of $1/\sqrt{5000} \approx 1.4\%$ for the generic sampling-error scale, although the exact variance of a Sobol estimator remains model dependent. In this study, the Sobol analysis is used primarily to identify and rank the dominant parameters rather than to report high-precision uncertainty bounds. Therefore, the sensitivity indices are interpreted comparatively, and the ranking of the highly sensitive parameters is the main design output.

Calculate the sensitivity of gear transmission dynamics model parameters.

It should be noted that not all parameters listed in Table 3 are statistically independent design variables. In particular, the equivalent moments of inertia J_1 and J_2 are physically related to the transmission ratios i_1 and i_2. According to the equivalent inertia relationship of the transmission system, $j_1 = j_3/({i_1}^2{i_2}^2)$ and $j_2 = j_3/{i_2}^2$. Therefore, J_1 and J_2 are not sampled independently in the Sobol analysis. For each Monte Carlo sample, the independent basic parameters are first generated according to their prescribed distributions, and the corresponding values of J_1 and J_2 are subsequently calculated from the sampled transmission ratios. In this way, the physical coupling between the transmission ratio and the equivalent moment of inertia is preserved during the sensitivity analysis.

Table 3. Probability distribution of gear transmission parameters.

Number	Parameter	Probability distribution	Parameter Value
1	$T_i/(N \cdot m)$	Uniform distribution	48-170
2	d/m	Normal distribution	0.022
3	m/kg	Normal distribution	236
4	B	Normal distribution	0.02
5	$k_s/(N \cdot m/rad)$	Uniform distribution	100-300
6	i_1	Uniform distribution	1-22
7	i_2	Uniform distribution	1-22
8	$J_1/(kg \cdot m^2)$	Derived parameter	$j_3/({i_1}^2{i_2}^2)$
9	$J_2/(kg \cdot m^2)$	Derived parameter	$j_3/{i_2}^2$
10	$J_3/(kg \cdot m^2)$	Normal distribution	0.028556

In addition, although the gear dimension and equivalent torsional stiffness may exhibit certain physical correlations in a detailed gear design, the equivalent stiffness k used in the present model represents the combined stiffness contribution of the gear-rack contact, transmission shafts, couplings, and other elastic components. Therefore, the gear diameter d and the equivalent stiffness k are treated as independent input parameters at the current modeling level. The influence of additional statistical correlations caused by manufacturing and assembly uncertainties will be further investigated in future work.

By analyzing the selection and design of gear transmission, combined with design experience and specific transmission requirements. Analyze the parameter values in the table and calculate the sensitivity values of each parameter, as shown in Figure 8.

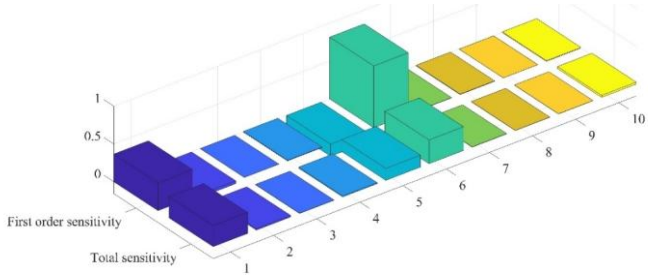


Figure 8. Sensitivity analysis results.

From the sensitivity results shown in Fig. 8, it can be seen that the input torque, stiffness, and transmission ratio corresponding to numbers 1, 5, and 6 are highly sensitive. When selecting and designing, it is important to focus on parameters with high sensitivity.

5. Dynamic stiffness simulation analysis and parameter matching of horizontal milling machine transmission system

5.1. Selection of optimal parameters for transmission systems

After completing the sensitivity analysis, use MATLAB/Simulink to establish a simulation model of the transmission system of the machine tool. By applying the MATLAB/Simulink functional module, debug the matching between different parameters and view the comparison output results.

For the transmission system of the new machine tool, when conducting dynamic analysis and optimization design of machine tool parameters, it is necessary to continuously analyze the overall dynamic characteristics of the transmission chain, conduct continuous analysis and simulation calculations through sensitivity models, and continuously improve the optimization design parameters based on feedback results, ultimately achieving the expected dynamic simulation purpose. Using MATLAB/Simulink for dynamic simulation of transmission systems and constructing simulation models of motor drive systems often requires general experimental data such as damping of feed transmission systems, as well as dynamic experimental data similar to machine tools or components.

5.2. Simulink simulation analysis verification

When selecting the natural frequency of the machine tool transmission system, select a natural frequency that is much greater than the overall state of the machine tool. Based on the actual operating speed of the machine tool and the motor speed, the initial selection of the motor model is 1FT7132-5AC7-1CG1, and the initial selection of the total transmission ratio i_t is 23, $i_t = i_1 i_2$.

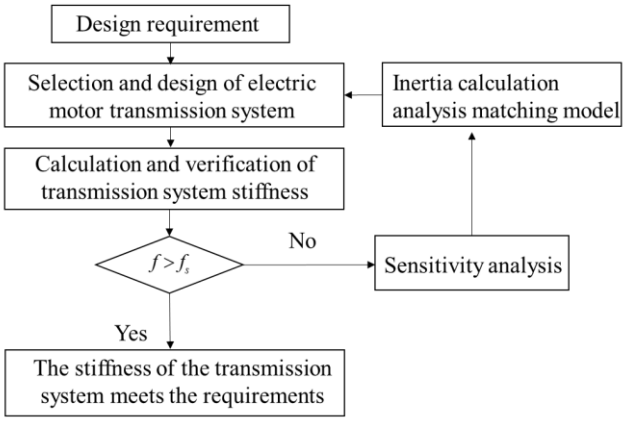


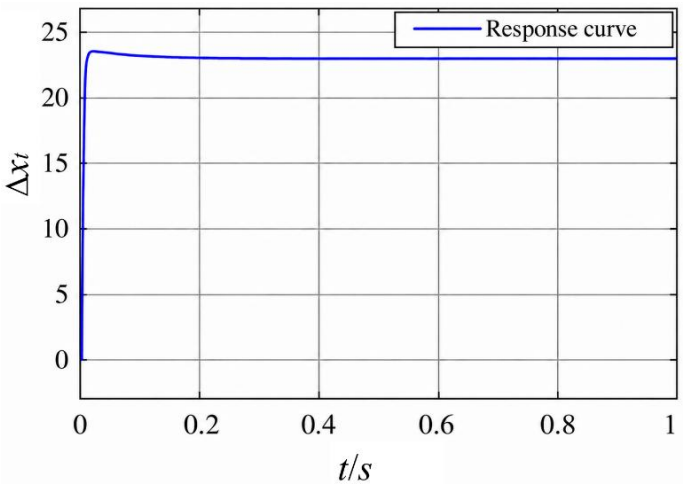
Figure 9. Model optimization feedback mechanism.

By selecting initial parameters, analyze the transmission system parameters of the machine tool, and obtain the response curve at the end of the transmission system by controlling the natural frequency and damping ratio of the transmission system in the dynamic equation, changing the gear rack contact backlash.

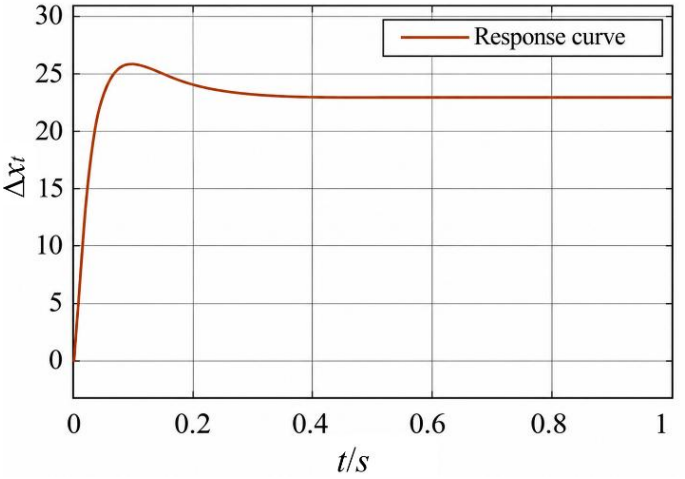
(1) Under a certain transmission ratio, changing the parameters of the machine tool transmission chain can obtain the Simulink simulation response curve. Keep the motor parameters unchanged and change the torsional stiffness.

1) Ensure that the transmission ratio remains unchanged and select rack and pinion transmission systems with different stiffness. The torsional stiffness of gear transmission is related to the backlash of rack and pinion transmission.

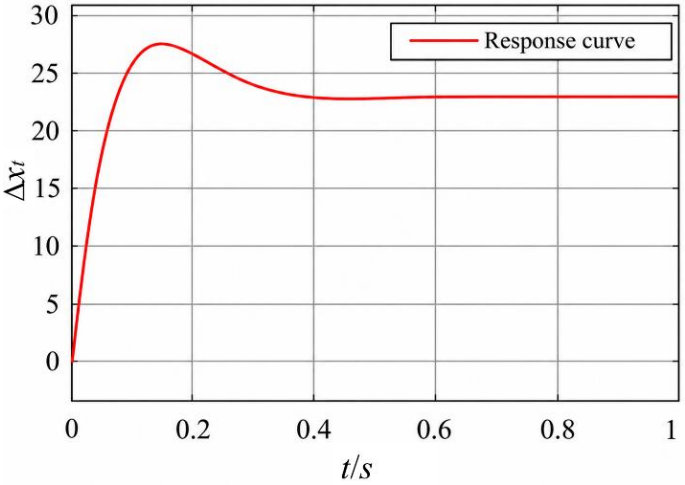
According to the Simulink simulation response curve in Figures 10, it can be seen that when the motor parameters and transmission ratio of the parallel system remain unchanged, high-precision gapless rack and pinion transmission, small backlash and large backlash gear transmission are selected respectively. The response curve in Figure 10 - (a) has a significantly higher step response speed than in Figures 10 - (b) and 10 - (c). The reduction of transmission backlash will significantly increase the torsional stiffness of the reducer, thereby reducing the vibration of the machine tool and improving its stability during the machining process.



(a) backlash-free



(b) low-backlash (0.25mm)



(c) large backlash (1.25mm)

Figure 10. Simulation curves of the transmission system under different backlash conditions of the rack-and-pinion transmission.

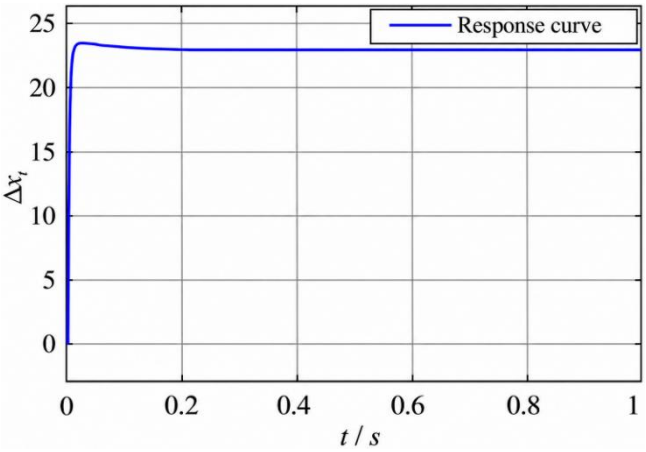
In the present Simulink model, the influence of rack-pinion clearance is represented by the corresponding change in equivalent torsional stiffness rather than by an explicit nonlinear dead-zone element. This approximation is appropriate for the nominal unidirectional feed condition considered here, in which the tooth flanks remain predominantly loaded on one side and the main effect of the clearance is reflected in the reduction of effective contact stiffness. During frequent motion reversal, however, backlash can introduce dead-zone behavior, impact and hysteresis, and the linear equivalent-stiffness model may underestimate the transient positioning error. Therefore, the comparison in Fig. 10 should be interpreted as a stiffness-oriented engineering assessment of different clearance levels. A nonlinear backlash/contact model will be required for a detailed reversal-transient analysis.

2) Ensure that the transmission ratio remains unchanged, select high-precision gapless gear transmission, compare the motor parameters and select different couplings to verify their stiffness, thereby indirectly changing the torsional stiffness, and compare it with the simulation response curve in Figure 10 - (a). Here, due to the requirements of machine tool speed and machining accuracy, rigid couplings, elastic couplings, and diaphragm type servo couplings are selected

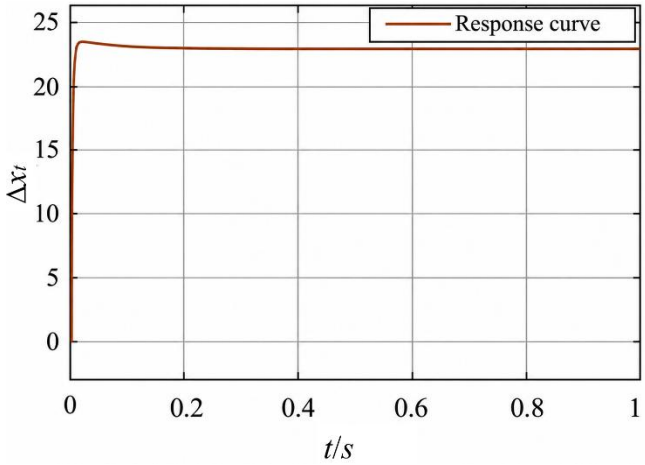
By comparing Figure 10 - (a) with Figures 11, it can be seen that the step response curve of the coupling changes less, but it can improve the stability of the machine tool to a certain extent. The diaphragm servo coupling in Figure 11 - (c) improves the step response speed of the transmission system better than the rigid coupling and elastic coupling, and has higher control accuracy. At the same time, the diaphragm type servo coupling has high torsional stiffness and a compact structure, which is very suitable for position accuracy control of mirror horizontal milling machine tools in aircraft skin processing. While driven by four motors, its good correction performance ensures the working life of adjacent connecting components and reduces the difficulty of machine tool dynamic balance adjustment.

(2) With the remaining parameters unchanged, change the values of ω_n and ξ and observe the system simulation curve. Firstly, select the initial undamped natural frequency based on the natural frequency of the machine tool, and analyze the response of the machine tool transmission system when ω_n and ξ are taken at different values according to the selection range of the machine tool.

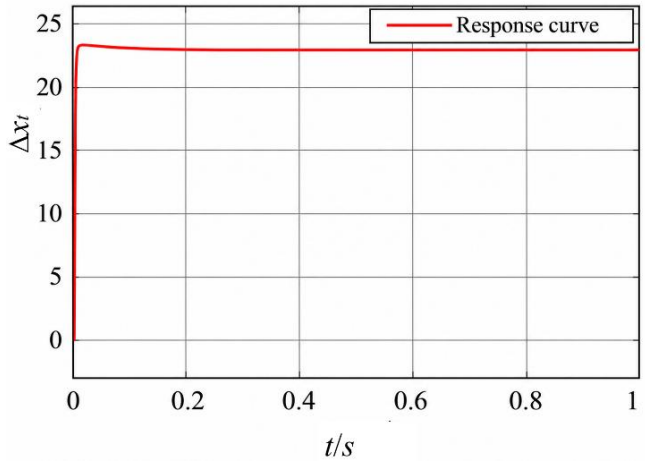
1) The natural frequency ω_n remains constant and the damping ratio ξ is changed.



(a) elastic coupling



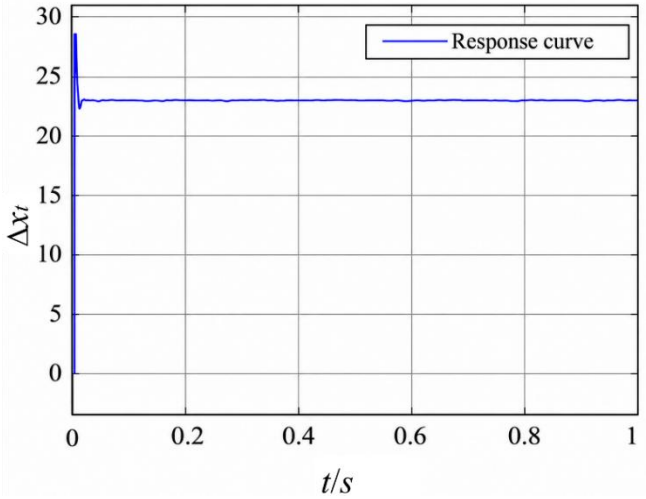
(b) rigid coupling



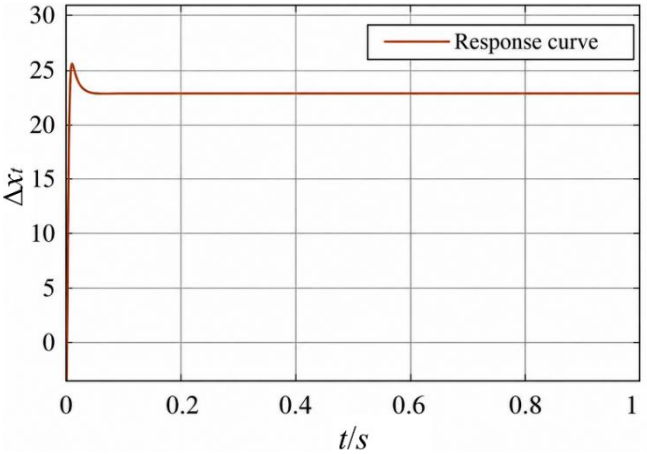
(c) diaphragm servo coupling

Figure 11. Simulation curves of the transmission system with different types of couplings.

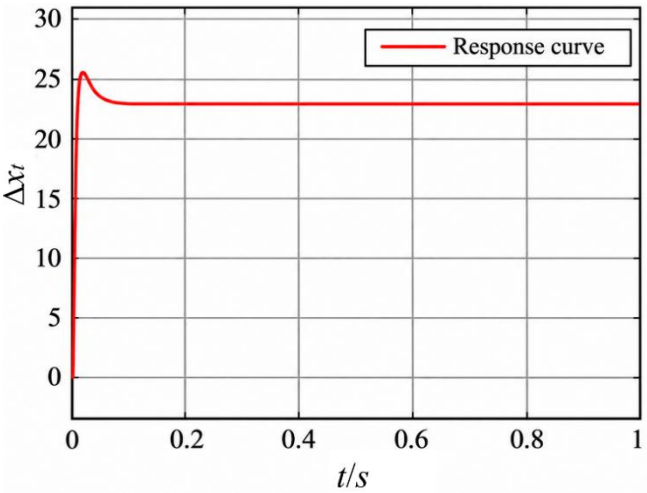
With the natural frequency and transmission ratio unchanged, reducing the damping ratio shortens the initial rise process but increases the tendency to overshoot and oscillate. Therefore, a lower damping ratio improves the apparent response speed at the expense of damping capability and response stability. For the mirror horizontal milling machine, both fast positioning and sufficient attenuation of oscillation are required. Based on the simulated responses, a damping-ratio range of $\xi = 0.03 - 0.06$ is selected as an engineering compromise between response speed and stability.



(a)

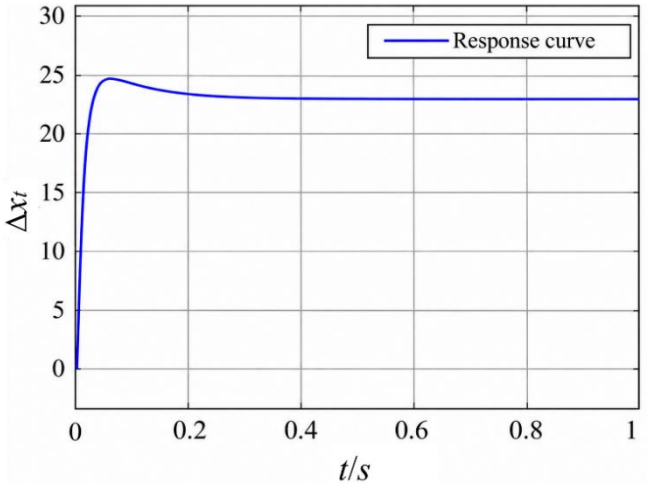


(b)

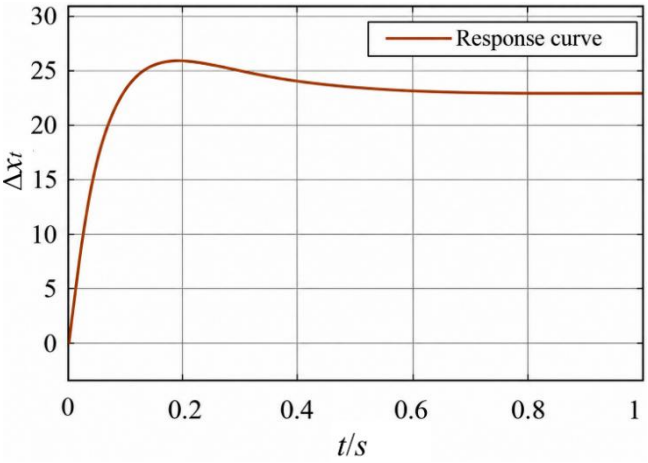


(c)

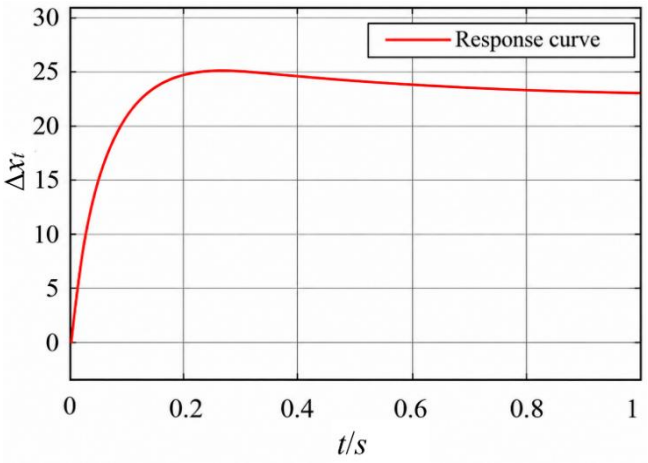
Figure 12. Simulation curve of the transmission system when $\xi = 0.015, \xi = 0.03, \xi = 0.06$.



(a) $\omega_n = 600$rad/s



(b) $\omega_n = 300$rad/s



(c) $\omega_n = 150$rad/s

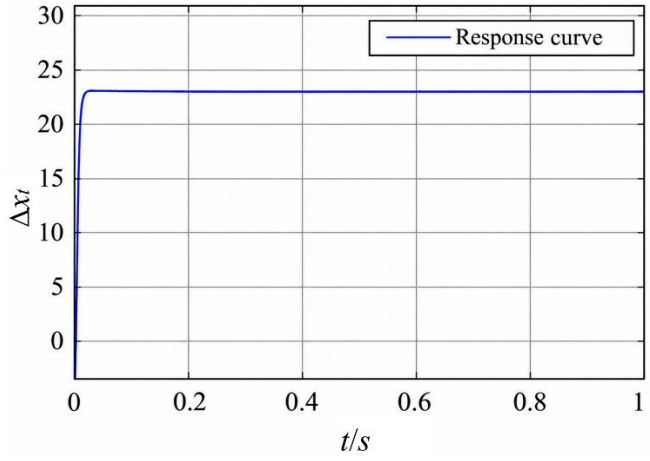
Figure 13. Simulation curve of the transmission system when$\omega_n = 600$,$\omega_n = 300$,$\omega_n = 150$rad/s.

2) Keep the damping ratio ξ constant, change the natural frequency ω_n value, and observe the system simulation curve.

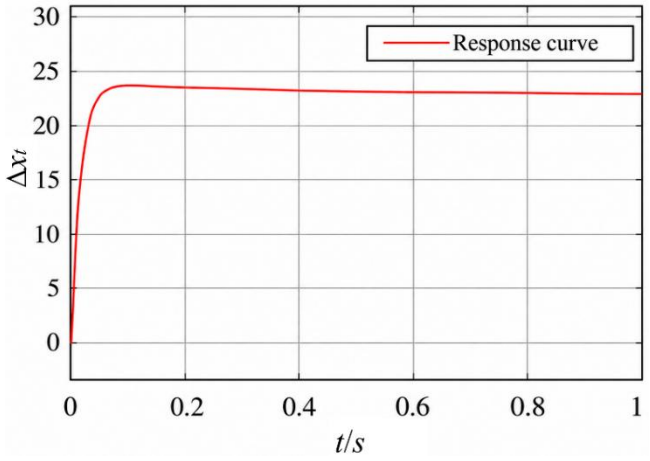
From the simulation curve, it can be seen that, while keeping the other parameters constant, the step response speed of the transmission system simulation curve improves significantly with the increase of the natural frequency ω_n. When selecting the natural frequency, consider that it is directly proportional to the square root of the equivalent stiffness coefficient k, and the damping ratio is inversely proportional to the square root of the equivalent stiffness coefficient k. Select these parameters appropriately to ensure that the machine tool operates with good speed and stability.

5.3. Transmission accuracy analysis

In the actual operation stage of the machine tool, a high-precision grating is added to the gear rack stage driven by the motor. The feedback of the grating is connected to the driving stage of the motor. While ensuring high accuracy in the reducer and coupling, the selection of motor speed and torque size will also affect the machining accuracy of the machine tool.



(a) Motor torque greater than load torque



(b) Motor torque less than load torque

Figure 14. Simulation curves of system dynamic response under different torque conditions.

Check the torque and speed of the motor. When the torque of the motor is small, the motor is not enough to support the

movement of the workbench, which will cause the entire transmission structure to shake, affecting the service life of the machine tool, reducing the reliability of the transmission system, and severely affecting the machining accuracy of the machine tool.

5.4. Joint parameter matching strategy

The sensitivity analysis and the single-factor response studies are combined into a coordinated parameter-matching procedure. The parameters with high global sensitivity, especially the input torque, equivalent torsional stiffness and transmission ratio, are treated as the primary matching variables, while the remaining quantities are constrained by component selection and kinematic relationships. First, the total transmission ratio i_t is selected according to the required feed speed and available motor torque. Second, the rack-pinion pair and coupling are selected to increase the equivalent torsional stiffness and reduce transmission backlash. Third, the damping ratio and natural frequency are jointly checked using $\xi = \frac{Bd^2}{2T\sqrt{k_s}}$ and $\omega_n = \sqrt{k_s/T}$ so that an increase in stiffness does not lead to an unacceptable oscillatory response. Finally, the selected motor is verified to provide a torque larger than the load torque. In the investigated design range, the coordinated solution therefore consists of i_t=23, a high-precision backlash-free rack-and-pinion transmission, a diaphragm servo coupling, ξ=0.03–0.06, and a natural frequency selected toward the upper part of the investigated range (300-600 rad/s) subject to stiffness, inertia and motor constraints.

6. Conclusion

This article conducts finite element modeling of the machine tool and analyzes the natural frequency of the machine tool and the deformation relationship of various components of the transmission system through LMS hammer vibration test. The dynamic and mathematical models of the transmission system were established, and sensitivity analysis was conducted on the parameters that affect the dynamic stiffness of the machine tool gear transmission system using the Sobol sensitivity analysis method. The dynamic characteristics of the transmission system were systematically identified.

The finite element modal results show good agreement with the hammer impact test results for the first three structural modes, with relative frequency errors of 3.511%, 3.147%, and 8.191%, respectively. The Sobol sensitivity analysis indicates that the input torque, equivalent torsional stiffness, and transmission ratio are the dominant parameters affecting the transmission response. The subsequent parameter-matching analysis demonstrates that a high-precision backlash-free rack-and-pinion drive and a diaphragm servo coupling can increase the effective stiffness and improve the dynamic response. A lower damping ratio results in a faster initial response but also leads to greater overshoot and oscillation; therefore, $\xi = 0.03 - 0.06$ is selected as a compromise between response speed and stability. Within the investigated range, increasing the natural frequency can improve the response speed; however, the motor torque must always remain higher than the load torque. By coordinating these factors, a practical sensitivity-guided parameter-matching strategy is obtained for the mirror horizontal milling machine. The current model is based on a nominal single-branch representation and a linearized treatment of transmission clearance. Multi-branch synchronization effects and nonlinear reversal dynamics will be considered in future work.

References

1. Wu ML, Yue XQ, Chen WB, Nie Q, Zhang Y. Accuracy analysis and synthesis of asymmetric parallel mechanism based on Sobol-QMC. *Proceedings of the Institution of Mechanical Engineers, Part C: Journal of Mechanical Engineering Science* 2020; 234(21): 4200-4214. https://doi.org/10.1177/0954406220920702.
2. Brassitos E, Jalili N. Dynamic model development and characterization of gear bearing transmission systems: theory and experiments. *IEEE/ASME Transactions on Mechatronics* 2019; 24(4): 1651-1661. https://doi.org/10.1109/TMECH.2019.2916333.
3. Franco O, Beudaert X, Ulacia I, Erkorkmaz K, Munoa J. Static stiffness analysis of an electronically preloaded rack and pinion feed drive system. *Procedia CIRP* 2025; 132: 68-73. https://doi.org/10.1016/j.procir.2025.01.012.
4. Wu S, Yu P, Yu T, Li M, Yang Z. Research on the evaluation method of dynamic characteristics of the feed system of double-pendulum five-axis machine tool. *Journal of Mechanical Science and Technology* 2025; 39(5): 2489-2505. https://doi.org/10.1007/s12206-025-0409-

9.
5. Quan L, Zhao W. A review on positioning uncertainty in motion control for machine tool feed drives. *Precision Engineering* 2024; 88: 428-448. https://doi.org/10.1016/j.precisioneng.2024.03.003.
6. Ostad Ali Akbari V, Schuppisser C, Kuffa M, Wegener K. Automated machine tool dynamics identification for predicting milling stability charts in industrial applications. *The International Journal of Advanced Manufacturing Technology* 2024; 130(11-12): 5879-5893. https://doi.org/10.1007/s00170-024-12952-x.
7. Verl A, Steinle L. Adaptive compensation of the transmission errors in rack-and-pinion drives. *CIRP Annals* 2022; 71(1): 345-348. https://doi.org/10.1016/j.cirp.2022.03.026.
8. Berthold J, Regel J, Dix M, Drossel WG. Operational modal analysis used to identify dynamic behaviour of machine tools during milling. *Procedia CIRP* 2023; 118: 128-133. https://doi.org/10.1016/j.procir.2023.06.023.
9. Liu YP, Altintas Y. Predicting the position-dependent dynamics of machine tools using progressive network. *Precision Engineering* 2022; 73: 409-422. https://doi.org/10.1016/j.precisioneng.2021.10.010.
10. Sato R, Noguchi S, Hokazono T, Nishida I, Shirase K. Time domain coupled simulation of machine tool dynamics and cutting forces considering the influences of nonlinear friction characteristics and process damping. *Precision Engineering* 2020; 61: 103-109. https://doi.org/10.1016/j.precisioneng.2019.10.010.
11. Franco O, Beudaert X, Erkorkmaz K, Munoa J. Feed drive control and non-linear friction interaction effect on machining chatter stability prediction. *Journal of Manufacturing and Materials Processing* 2024; 8(5): 207. https://doi.org/10.3390/jmmp8050207.
12. Brecher C, Fey M, Tenbrock C, Daniels M. Multipoint constraints for modeling of machine tool dynamics. *Journal of Manufacturing Science and Engineering* 2016; 138(5): 051006. https://doi.org/10.1115/1.4031771.
13. Grossi N, Sallese L, Montevecchi F, Scippa A, Campatelli G. Speed-varying machine tool dynamics identification through chatter detection and receptance coupling. *Procedia CIRP* 2016; 55: 77-82. https://doi.org/10.1016/j.procir.2016.08.022.
14. Beudaert X, Franco O, Erkorkmaz K, Zatarain M. Feed drive control tuning considering machine dynamics and chatter stability. *CIRP Annals* 2020; 69(1): 345-348. https://doi.org/10.1016/j.cirp.2020.04.054.
15. Lin L, He M, Wang Q, Deng C. Chatter stability prediction and process parameters' optimization of milling considering uncertain tool information. *Symmetry* 2021; 13(6): 1071. https://doi.org/10.3390/sym13061071.
16. Rao C, Xu L, Chen Q, Ye W. Dynamic modeling and performance evaluation of a 2UPR-PRU parallel kinematic machine based on screw theory. *Journal of Mechanical Science and Technology* 2021; 35(6): 2369-2381. https://doi.org/10.1007/s12206-021-0509-0.
17. Guo Z, Cheng Q, Zhang H, Niu P, Zhang C, Liu Z. Error analysis model and optimization method for guideway assembly based on elastic interaction effects. *Applied Mathematical Modelling* 2026; 156: 116774. https://doi.org/10.1016/j.apm.2026.116774.
18. Lin WZ, Wu KD, Shih WC, Hung JP. A computer-experimental approach to modeling the machine tool dynamics including the effect of spindle bearing preload. *DEStech Transactions on Computer Science and Engineering* 2018. https://doi.org/10.12783/dtcse/ccme2018/28569.
19. Deng C, Liu Y, Zhao J, Wei B, Yin G. Analysis of the machine tool dynamic characteristics in manufacturing space based on the generalized dynamic response model. *The International Journal of Advanced Manufacturing Technology* 2017; 92(1–4): 1411-1424. https://doi.org/10.1007/s00170-017-0201-9.
20. Xu C, Gertner G. Extending a global sensitivity analysis technique to models with correlated parameters. *Computational Statistics & Data Analysis* 2007; 51(12): 5579-5590. https://doi.org/10.1016/j.csda.2007.04.003.
21. Guo F, Li C, Su J, Liu C. Study on dynamic uncertainty and sensitivity of gear system considering the influence of machining accuracy. *Applied Sciences* 2023; 13(14): 8011. https://doi.org/10.3390/app13148011.
22. Li M, Wang S, Ma C, Xia C. Identification of key errors for large-sized gear hobbing machines based on tooth surface posture-geometric error model. *China Mechanical Engineering* 2023; 34(5): 533-542. https://doi.org/10.3969/j.issn.1004-132X.2023.05.004.
23. Li X, Yuan J, Wang Z. Optimal design method for geometric errors of horizontal machining center based on Sobol method and IPSO. *The International Journal of Advanced Manufacturing Technology* 2024; 131(11–12): 6091-6102. https://doi.org/10.1007/s00170-024-13097-7.
24. He S, Shi T. Sensitivity analysis of surface contour error to geometric errors for four-axis ultra-precision machine tools. *Journal of*

Manufacturing Processes 2024; 131: 569-588. https://doi.org/10.1016/j.jmapro.2024.09.053.

25. Navid A, Khalilarya S, Abbasi M. Diesel engine optimization with multi-objective performance characteristics by non-evolutionary Nelder-Mead algorithm: Sobol sequence and Latin hypercube sampling methods comparison in DoE process. *Fuel* 2018; 228: 349-367. https://doi.org/10.1016/j.fuel.2018.04.142.
26. Yang H, Shi W, Guo L, Zhao Y, Yuan R. Study on mesh stiffness and sensitivity analysis of planetary gear system considering the deformation effect of carrier and bearing. *Engineering Failure Analysis* 2022; 135: 106146. https://doi.org/10.1016/j.engfailanal.2022.106146.
27. Liu L, Ma G, Jiang X, Cao Z, Zhang W, Shang K, Jin X. Error analysis method and sensitivity analysis for linkage transmission mechanism. *Journal of Physics: Conference Series* 2021; 1939(1): 012033. https://doi.org/10.1088/1742-6596/1939/1/012033.
28. Zhang L, Zong X, Tang Y, Chen X, Feng J, Yuan X. Modal and natural frequency sensitivity analysis of electrohydraulic Stewart platform. *Shock and Vibration* 2021; 2021(1): 5587282. https://doi.org/10.1155/2021/5587282.
29. Zhao R, Huang H, Mei L. A method for constructing digital twins of CNC machine tools feed systems based on hybrid mechanism-data. *Scientific Reports* 2025; 15(1): 32186. https://doi.org/10.1038/s41598-025-17587-w.